Automated Three-Dimensional Detection of Intracoronary Stent Struts in Optical Coherence Tomography Images

Nico Bruining, Kenji Sihan, Jurgen Ligthart, Sebastiaan de Winter, Evelyn Regar

Erasmus MC, Thoraxcenter, Rotterdam, The Netherlands

Abstract

Optical coherence tomography (OCT) is a new intracoronary imaging tool that has been recently introduced and has become the method of choice to investigate new treatment methods for coronary artery disease. Due to the OCT's high image resolution, hundreds of stent struts are visualized per patient and therefore a computer-assisted stent strut detection method could help to improve accuracy by reducing analysis time.

An automated strut detection algorithm was developed based on an adapted K-nearest neighbor method. Validation in stent just implanted resulted in a success rate of 77%. In a stent follow-up group (n=14) 6 months after implantation with tissue growth a success rate of 50% was observed.

Computer-assisted stent strut detection in OCT images is well feasible in patients directly after implantation; in case of considerable tissue growth it is more challenging.

1. Introduction

Optical coherence tomography (OCT) has been recently introduced as a new intracoronary imaging tool. It is capable of acquiring cross-sectional images of the coronary vessels at resolutions which previously were only possible by histopathology and microscopy. Its resolution is much higher than that of intravascular ultrasound (IVUS) the current reference method for intracoronary imaging. Due to its excellent resolution OCT could potentially serve as a research tool to evaluate the results of new interventional therapies and more especially new stent designs [1]. The visualization of stent struts has shown to be excellent by OCT (Fig. 1). By applying OCT observers can evaluate if the stent is well expanded against the coronary vessel wall directly after implantation [2]. The visualization of stent struts has shown to be excellent by OCT. Furthermore, during follow-up examinations coverage of the stent by tissue can be evaluated. An important topic as in the recent past is has been shown that uncovered drug-eluting metallic stents (DES) could potentially result in adverse effects for the patients such as acute stent thrombosis after cessation of anti-thrombotic medication.

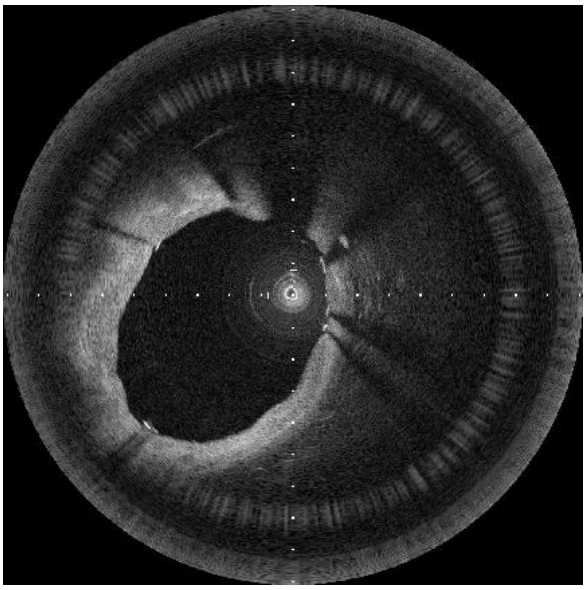

Figure 1. An example of a cross-sectional OCT image with stent struts, which are visible as white rims followed by a shadowing tail.

Due to its high-resolution many details of the stents are present into the cross-sectional images resulting in hundreds of visible stent struts in each pullback per patient. Identifying all these struts manually results in a time-consuming and tedious analysis process. As the struts are well visible the hypothesis was that an automated tool could be helpful in this analysis process as other automated detection algorithms such as the detection of the lumen-intima interface contours have shown to be successful in the recent past [3, 4].

2. Methods and materials

OCT imaging was performed by a commercially frequency domain OCT (FD-OCT) available system (St. Jude/Lightlab imaging Inc, Westford, MA, USA) [5]. The system uses a 1310-nm broadband light-source generated

by a super luminescent diode with an output power of 8.0mW. The average tissue penetration depth is approximately 1.5 mm with an axial and lateral resolution of 15 µm and 25 µm, respectively. The imaging probe has the size of a guide-wire with a maximum outer diameter of 0.014 inch (LightLab Imaging). The wire contains a single-mode fibre optic core within a translucent sheath. It is connected to an imaging console, similar to ICUS, that is responsible for real-time image data processing, visualization and image storage. Systematic imaging of a coronary segment is also similar to ICUS by an automatic continuous speed pullback but at much higher speeds, e.g. between 20 to 40 mm/s, of the imaging wire. OCT images are generated at a rate of >100 frames/ second (in comparison: ICUS 30 frames/s).

2.1. Patient populations

OCT images for development and later validation were acquired from two different cohorts of patients: 1) 15 patients were imaged directly after stent implantation and 2) 14 patients were imaged during a follow-up examination mostly after 6-months' time period. These two cohorts result in different imaging characteristics as during this 6 months period vascular healing results in tissue coverage of the stent struts resulting in different imaging characteristics.

2.2. Stent strut detection algorithm

During pullback OCT catheter emits and collects the reflected coherent infra-red light to acquire information about the vessel wall. The vessel wall is imaged and sequence of images is produced. Every cross-section shows a slice of the vessel wall, with the catheter at the center surrounded by vessel tissue and sometimes metal struts followed by a shadow trail. OCT cross-sections often contain noise and artifacts. Before further processing these are filtered to improve the accuracy of our metal stent detection algorithm. In the cross-sections an image overlay is often present that contains high intensity pixels. This overlay may vary from dataset to dataset and multiple bright pixels can be clustered next to each other.

The following algorithm is used to remove the overlay:

```
for k from 1 to N
        I' = erosion_filter(I)
        I = replace_threshold(I, I', T)
end
```

where *I* is the input image, *T* is a threshold (chosen such that is it just below the intensity value of the overlay), *erosion_filter* is a 3x3 erosion filter and *replace_threshold* is a function that for every pixel in *I* above *T* replaces it with the value from *I'*. This algorithm erodes only the overlay and effectively removes it from the cross-section while not affecting the rest of the image.

For our application we convert every cross-section to polar coordinates (Fig 2). In polar coordinates the rows and columns contain angular and depth information between the vessel wall and the catheter. The rows of the polar images represent the angle in Cartesian coordinates and the columns represent the depth information. A metal stent in this polar converted image appears as a small bright spot and a dark trail to the right of this bright spot.

Figure 2. Masking, noise-filtering and transformation to polar coordinates.

To find the depth location of a metal stent we take the maximum of a row (Fig. 3).

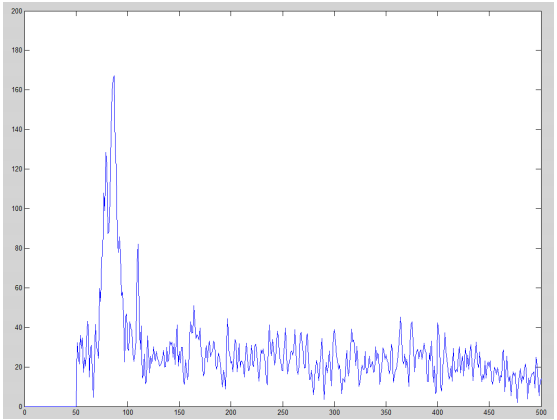

Figure 3. Example of row intensity containing a stent without noise filtering. The maximum intensity is at the location of the peak.

The maximum of a row determines the location of the stent because the metal stents are highly reflective compared to tissue. The peak of a row containing a stent should be exactly at the part where the infra-red light is

reflected. Every row is transformed into a feature vector. The feature vector consists of the following features:

- Mean
- Maximum
- Sum of values above mean

The mean is chosen because a row containing a strut will have a lower mean than rows without a strut. Struts cast a shadow because they block infra-red light; this has the effect of lowering the mean intensity of a row. Due to the reflective properties of metal struts with infrared-light the maximum greatly increases compared to the vessel wall. The sum of values above the mean is very small for rows that contain a strut because the intensity of only a small part of the row is above the mean.

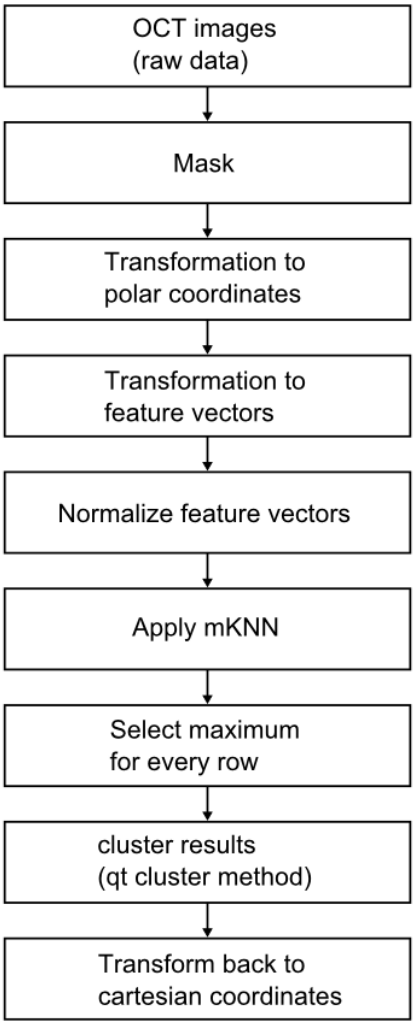

Figure 4. An overview of the strut detection algorithm.

Each feature on its own is not accurate enough to decide if a row is part of a strut or not. Combining all features increases the accuracy for classification. The distribution of the values of every feature has to be normalized to avoid an unequal weight attribution among the features.

The normalization step is applied to every feature as follows:

$$\frac{x - mean(x)}{std(x)},$$

Where *mean* is the mean of the sequence and *std* is the standard deviation.

Detecting struts within a cross-section that is transformed to polar coordinates is a matter of selecting the rows at the position of the struts. A row may either be part of a strut or it is not. Separating rows into classes is a classification problem. We solved this classification problem with a modified K-nearest neighbor (mKNN) algorithm. The mKNN with a-priori information is applied to all rows to find a solution for this classification problem. The a-priori information consists of five manually selected frames that we considered visually diverse enough to detect most of the struts. Struts often span multiple rows; these rows are clustered with a qt clustering algorithm to select one row per stent.

In some cases the stent detection algorithm is not capable of detecting a strut due to image artifacts and noise. To correct for this a manual review of the cross-sections is required. Our software allows for stepping through every frame and manually add or remove struts where required. Figure 4 shows a schematic overview of the algorithm.

3. Validation

A total of 29 OCT datasets were analyzed containing a total of 4024 frames. In the post-implant group (n=15), 23608 struts were detected of which 3626 had to be removed, 115 moved and 1155 had to be added, resulting in a success rate of 77% for the algorithm. In the follow-up group (n=14), a total of 21077 struts were detected of which 5749 struts had to be removed, 1008 moved and 1915 added, resulting in a success rate of 50%. The average analysis time (automated plus correction), was on average 4.1 sec/frame for the post-implant and 6.3 sec/frame for the follow-up population.

4. Discussion

Automated, or perhaps better stated computer-assisted, detection of metallic coronary stent struts of stents imaged by OCT directly after implantation seems feasible. A success rate of almost 80% is a score which could be expected in human medical image data. A 100% score is for most automated algorithms in medical image processing almost impossible to reach. The 50% success rate of strut detection of stents which are covered by a

layer of tissue seems on first sight a bit disappointing. However, we encountered several issues which explain for the larger part this drop in success. 1) The penetration power of OCT is limited, therefore thick layers of tissue causes that the stent struts are not showing the peak intensity similar to those not covered by tissue, as can be observed in figure 3. 2) Due to the clustering necessary for implementation of this algorithm, sometimes two struts which by the algorithm are detected as one are indicated by the expert as 2. 3) The applied guide-wire caused an artifact resulting in the detection of 2 extra struts in every image which needed manual correction. 4) Coronary anatomies such as large side-branches could cause problems for an appropriate detection of the stent struts.

Several other publications are claiming that they developed a fully automated algorithm with a high success rate [6, 7]. However, in all of these publications, the validation of these fully-automated algorithms has only been tested on a limited number of individual cross-sections. This makes it difficult, if not impossible to compare the efficacy of these different algorithms. A possible solution to overcome this problem could be a central database in which a number of OCT acquisitions is present and of which the human expert analyses data is also available. If such a database would be accessible by developers than they could test their algorithms and those outcomes of different development groups could be compared.

4.1. Future developments

Of course there is always something that could be improved. The algorithm could be further enhanced and modified to result in higher success rates. Incorporation of this algorithm into standard OCT analysis software is the next step to improve user acceptance and ease of use. Another important clinical request is, if it would also be possible to automatically, or computer-assisted, detect the amount of tissue present inside the stent. This could then be used to compare different new DES platforms against each other [1]. As OCT is limited in tissue penetration depth, IVUS is still the de facto imaging technique of choice if one wants to study the effects of different types of DES platforms over time onto the tissue composition and its changes of the stented region.

As OCT is limited in tissue penetration depth, IVUS is still the de facto imaging technique of choice if one wants to study the effects of different types of DES platforms over time onto the tissue composition and its changes of the stented region.

However, as IVUS has a limited resolution, effects of the stent or drug on the stent in the stent-intima interface could be better studied by OCT. The optimal situation would therefore be to superimpose the image data sets of both modalities acquired in the same stented segment.

5. Conclusion

Computer-assisted stent strut detection in OCT images is well feasible in patients directly after implantation. In patients who showed considerable tissue growth inside their stents at follow-up it is more challenging. However, the current proposed method can save considerable analysis time and helps to improve the accuracy.

References

[1] Regar E, Ligthart J, Bruining N, van Soest G. The diagnostic value of intracoronary optical coherence tomography. Herz. 2011 Aug;36(5):417-29.

[2] Regar E, van Soest G, Bruining N, Constantinescu AA, van Geuns RJ, van der Giessen W, et al. Optical coherence tomography in patients with acute coronary syndrome. EuroIntervention. 2010 May;6 Suppl G:G154-60.

[3] Sihan K, Botha C, Post F, de Winter S, Gonzalo N, Regar E, et al. Fully automatic three-dimensional quantitative analysis of intracoronary optical coherence tomography: method and Validation. Catheter Cardiovasc Interv. 2009 Dec 1;74(7):1058-65.

[4] Sihan K, Botha CP, Post FH, de Winter S, Regar E, Hamers R, et al. A Novel Approach to Quantitative Analysis of Intravascular Optical Coherence Tomography. Computers In Cardiology. 2008;35:1089-92.

[5] Okamura T, Gonzalo N, Gutierrez-Chico JL, Serruys PW, Bruining N, de Winter S, et al. Reproducibility of coronary Fourier domain optical coherence tomography: quantitative analysis of in vivo stented coronary arteries using three different software packages. EuroIntervention. 2010 Aug;6(3):371-9.

[6] Ughi GJ, Adriaenssens T, Onsea K, Kayaert P, Dubois C, Sinnaeve P, et al. Automatic segmentation of in-vivo intra-coronary optical coherence tomography images to assess stent strut apposition and coverage. Int J Cardiovasc Imaging. 2011 Feb 24.

[7] Unal G, Gurmeric S, Carlier SG. Stent implant follow-up in intravascular optical coherence tomography images. Int J Cardiovasc Imaging. 2010 Oct;26(7):809-16.

Address for correspondence:

Nico Bruining, PhD
Erasmusmc MC, P.O. Box 1738,
3000 DR Rotterdam, The Netherlands,
Tel: +31107033934
Email: n.bruining@erasmusmc.nl